JOURNAL OF SPACECRAFT AND ROCKETS
Vol. 42, No. 3, May–June 2005

Thermal Design of Liquid Droplet Radiator for Space Solar-Power System

Tsuyoshi Totani,* Takuya Kodama,† Harunori Nagata,‡ and Isao Kudo§
Hokkaido University, Hokkaido 060-8628, Japan

The waste heat from the space solar-power system, which supplies 5 MW of electricity to a power transmission line on Earth, is estimated, and the liquid droplet radiator for handling the waste heat are examined on the basis of experimental results obtained under microgravity for droplet generation and droplet collection of the liquid droplet radiator. The following results have been obtained. First, an active heat removal system for the power generation unit in the photovoltaic power system is not necessary when the concentration ratio of solar energy is smaller than 1.34, whereas for the liquid droplet radiator, with silicon oil as working fluid, in the solar dynamic power system, the droplet sheet for radiating the waste heat must be 147 m long, 65.1 m wide, and 0.998 m thick. Second, the droplet sheet of the liquid droplet radiator, in which the working fluid is silicon oil, must be 107 m long, 43.2 m wide, and 0.998 m thick to manage the waste heat from the power distribution unit and the power transmission unit in the photovoltaic power system, whereas it must be 107 m long, 65.2 m wide, and 0.998 m thick in the solar dynamic power system.

Nomenclature

A = area, m^2
a = entrance length of a nozzle, $= 0.065$
C_a = transmittable energy per unit area perpendicular to the transmission direction, $= 2.3$ kW/m^2, W/m^2
C_r = concentration ratio
C_s = solar contact, W/m^2
c = specific heat of working fluid, J/(kg · K)
D = diameter of nozzle, m
d = diameter, m
dT = temperature interval, K
dt = time interval, s
dV = total volume of droplets, m^3
dx = traveling distance of droplets, m
E = energy transmitted per second, W
f = frequency of pressure disturbance, Hz
H = waste heat, W
H_1 = heat input per second, W
H_2 = heat output per second, W
h = thickness of a droplet sheet, m
k = nondimensional wave number, $= \pi Df/v_0$
L = length of nozzle, m
l = length of droplet sheet, m
$\dot{m}$ = mass flow rate of working fluid, kg/s
n = number density of droplets, 1/m^3
q = flow rate of working fluid, m^3/s
s = spacing, m
T = temperature, K
T_0 = temperature at the exit of droplet generator, K
$T_1 \sim T_6$ = temperatures at points of closed Brayton cycle, K
v_0 = velocity at the exit of nozzles, m/s
w = width of droplet sheet, m
x = distance from droplet generator, m
β = growth factor, 1/s
ΔH = thermal energy lost per second of working fluid, W
ΔP = pressure difference between inside and outside of droplet generator, Pa
ΔT = temperature difference between droplet generator and droplet collector, K
ε = emissivity
η = efficiency
ξ = coefficient of pressure loss in the entrance region of nozzle, $= 2.3$
ν = kinematic viscosity of working fluid, m^2/s
ρ = density, kg/m^3
σ = Stefan–Boltzmann constant, $= 5.67 \times 10^{-8}$, W/($m^2 \cdot K^4$)
τ = optical depth normal to the surface of droplet sheet

Subscripts

a = antenna
CBC = closed Brayton cycle
c = concentrator
d = droplet
d-t = power distribution unit and power transfer unit
LDR = liquid droplet radiator
n = nozzle
PV = photovoltaic power system
sa = solor array
SD = solor dynamic power system
sheet = droplet sheet

Introduction

THE space solar-power system (SPS)[1,2] generates electric power in orbit, converts the power into microwaves, and then transmits the microwaves to Earth. The SPS can generate electric power regardless of the weather, can utilize the inexhaustible solar energy, and does not release carbon dioxide in the process of power generation. The SPS is being considered as an alternative power generation system that is able to supply electric power semipermanently and stably in an environmentally friendly manner.

However, discarding the large quantities of waste heat is one of the technical issues that must be considered to realize large space

Received 6 February 2003; accepted for publication 1 May 2004.

*Research Associate, Graduate School of Engineering, Division of Mechanical Science, Kita 13 Nishi 8, Kita ku, Sapporo; tota@eng.hokudai.ac.jp. Member AIAA.
†Graduate Student, Graduate School of Engineering, Division of Mechanical Science, Kita 13 Nishi 8, Kita ku, Sapporo.
‡Associate Professor, Graduate School of Engineering, Division of Mechanical Science, Kita 13 Nishi 8, Kita ku, Sapporo.
§Professor, Graduate School of Engineering, Division of Mechanical Science, Kita 13 Nishi 8, Kita ku, Sapporo. Member AIAA.

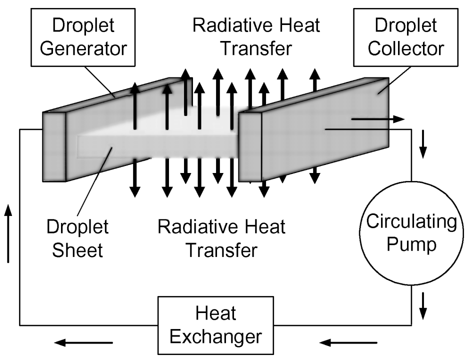

Fig. 1 Schematic diagram of liquid droplet radiator.

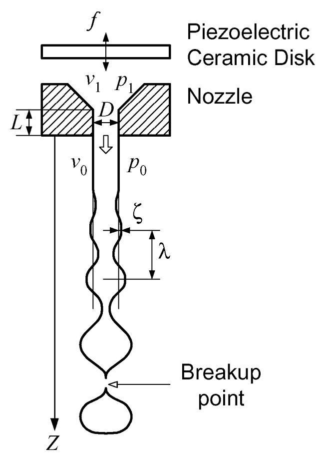

Fig. 2 Transformation process from a jet to droplets.

structures that handle high power (from megawatt to gigawatt order), such as the SPS. The liquid droplet radiator (LDR) is an important candidate for resolving this issue. Its lightweight structure, high resistance to meteorite impacts, small storage volume requirement at launch, and easy deployment in space make it a very attractive heat removal system for the SPS.

The operation of the LDR is schematically shown in Fig. 1. The LDR, which consists of a droplet generator, a droplet collector, a circulating pump, and a heat exchanger, circulates working fluid as follows. The working fluid is heated through a heat exchanger by the waste heat generated in a large space structure. Then, the working fluid is subjected to a pressure disturbance generated by a piezoelectric vibrator in the droplet generator and is emitted into space through nozzles on the droplet generator toward a droplet collector. At some distance from the droplet generator, the working fluid is atomized into multiple streams of liquid droplets by the growth of the radial disturbance amplitude caused by the pressure disturbance increases, as shown in Fig. 2. During the transport in space from the droplet generator to the droplet collector, the droplets lose thermal energy via radiative heat transfer. After the cooled droplets are captured by the droplet collector, the working fluid is recycled to the heat exchanger by a circulating pump.

Liquids with low vapor pressure are nominated as candidates of working fluids from the viewpoint of minimizing evaporation loss. These liquids include silicon oils for the waste heat temperature range of 250–350 K, liquid metal eutectics for 370–650 K, and liquid tin for 500–1000 K (Ref. 3). Because LDRs do not require solid bodies to protect the radiating surface from puncture by small particles such as debris or small meteorites, they are lightweight, stowed in a small volume at launch, and easily deployed in orbit.[4] Taussig and Mattick[4] reported that LDRs can be as much as 5 to 10 times lighter than advanced heat pipe radiators. Massardo et al.[5] reported that the specific mass of a solar dynamic power system (SDPS) with an LDR is 27% less than that with a conventional heat pipe radiator. The droplet generation experiments and the droplet collection experiments on Earth have been conducted at the NASA John H. Glenn Research Center and the National Institute of Advanced Industrial Science and Technology in Japan.[6–9] The droplet generation experiments and the droplet collection experiments under microgravity using dropshafts have been carried out by the authors.[10,11]

In this study, we aim to estimate the amount of waste heat from an SPS that feeds 5 MW to a power transmission line on Earth and to consider the required size of the droplet sheet of the LDR to handle the waste heat. The size of the droplet sheet of the LDR is calculated on the basis of the results of the experiments performed under microgravity. Two power generation systems, the photovoltaic power system (PVPS) and the SDPS, have been regarded as models of the SPS in this study.

Microgravity Experiments

Performance tests of the LDR elements have been carried out under microgravity by using two dropshafts in Japan: Japan Microgravity Center Co., Ltd., and Micro-Gravity of Japan Co., Ltd. The conditions under which the LDR functions properly in a microgravity environment have been clarified from these tests.

Droplet Generator

Images of droplets under the microgravity condition are shown in Fig. 3. The pressure difference between the inside and outside of the droplet generator is 0.48 MPa, and the disturbance frequency is 20 kHz. These images clearly proved that a droplet stream is also produced under the microgravity condition and that the diameter of droplets and the spacing between droplets are uniform. The diameter of droplets has been measured as 220 μm from these images. Also, the spacing between droplets has been measured as 500 μm.

Figure 4 shows growth factor β vs nondimensional wave number k of the pressure disturbance.[8,10,12] In this figure, the experimental conditions of Figs. 3, 5a, and 5b are also plotted. A uniform stream of droplets of uniform diameter and spacing is generated on Earth in the range denoted by the bold section of the curve in Fig. 4 (Ref. 7). Uniform droplet streams have been observed under the conditions marked by the open circles except for Fig. 5b in microgravity environments.

It has been clarified from the microgravity experiments on the droplet generator that the diameter of droplets and spacing between droplets generated under microgravity can be predicted by the following equations based on the law of conservation of mass[9]:

$$d_d = (3\pi/2k)^{\frac{1}{3}} D \tag{1}$$

$$s_d = (\pi/k)D - (3\pi/2k)^{\frac{1}{3}} D \tag{2}$$

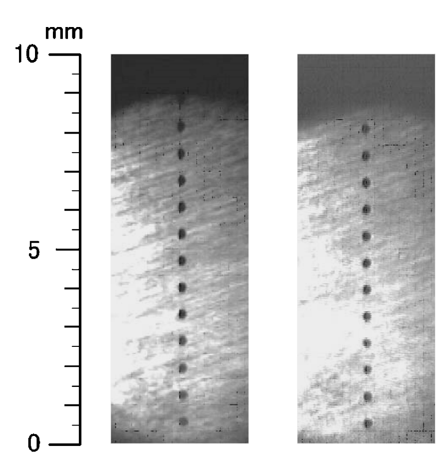

Fig. 3 Images of droplets under normal gravity and microgravity (ΔP = 0.48 MPa, f = 20 kHz): black spherical shades are droplets.

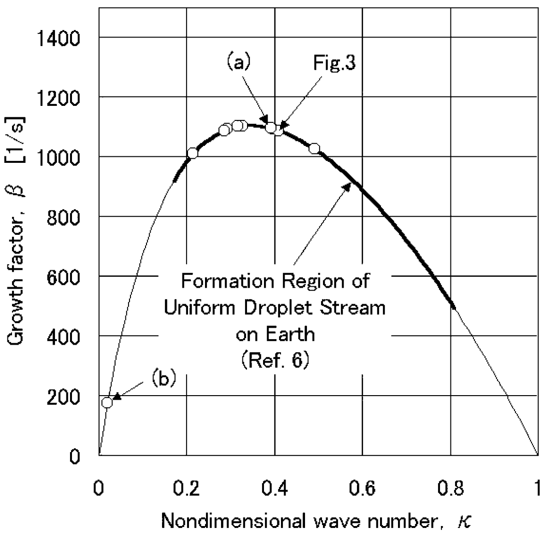

Fig. 4 Growth factor vs nondimensional wave number.

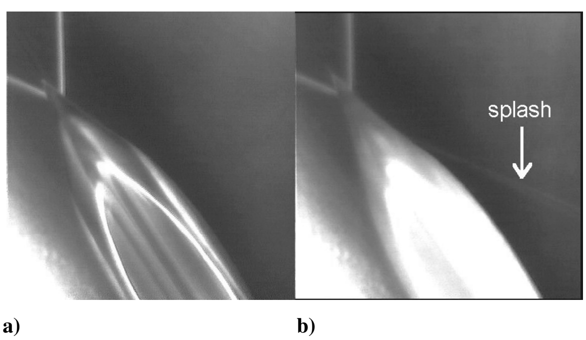

Fig. 5 Collisions of droplet stream: a) uniform droplet stream and b) nonuniform droplet stream.

Droplet Collector

Figure 5 shows images for a) a uniform droplet stream and b) a nonuniform droplet stream colliding against an aluminum board with an incidence angle of 35 deg. The pressure difference between the inside and outside of the droplet generator in Figs. 5a and 5b is 0.50 MPa, resulting in a droplet velocity of 16 m/s. The disturbance frequency in Fig. 5a is 20 kHz, resulting in a droplet diameter of 250 μm, while the disturbance frequency in Fig. 5b is 1 kHz. As the images show, splashing of working fluid does not occur in Fig. 5a, whereas splashing takes place in Fig. 5b. It is clear from Fig. 4 that a nonuniform droplet stream is produced on Earth in case (b). Because it has been reported that there are larger droplets in the nonuniform droplet stream than those in the uniform droplet stream,[9] splashing on the aluminum board in Fig. 5b has been believed to be caused by the larger droplets in the nonuniform droplet stream.[11] In this study, the LDR is designed in such a way that the growth factor β is approximately the maximum value in order to generate the uniform droplet stream.

SPS Model

PVPS model

The concept of the PVPS is schematically shown in Fig. 6. The solar cell of this model is a single crystal of silicon, the power generation efficiency of which is expected to reach 85% of the theoretical efficiency of single-crystal silicon in space use in the near future. Table 1 shows the efficiency, the input energy, and the waste heat of each component in the PVPS.[13] In the power generation unit, the cell efficiency, the deterioration of the cell efficiency caused by temperature, the array design factor, and aging degradation (30 years) are taken into account. A large area of the solar array is necessary to receive the input energy per second H_{1sa} of 61.6 MW. As the solar constant in Earth orbit is $C_s = 1.37$ kW/m^2, the required area of the

Table 1 System efficiency chain of PVPS

Item	Efficiency	Input energy, MW	Waste heat, MW
Solar cell	0.220	61.59	48.04
Efficiency deterioration caused by temperature	0.954	13.55	0.62
Array design factor	0.951	12.93	0.63
Aging degradation (30 years)	0.800	12.29	2.46
Power converter and booster	0.950	9.83	0.49
Pantographic cables and distribution cables	0.990	9.34	0.09
Rotary joint	0.990	9.25	0.09
Power source of the transmission device	0.950	9.16	0.46
dc-rf conversion	0.800	8.70	1.74
Antenna	0.965	6.96	0.24
Atmosphere	0.980	6.72	0.13
Energy collection	0.890	6.58	0.72
rf-dc conversion	0.880	5.86	0.70
Grid interface	0.970	5.15	0.15
Powerline	——	5.00	——

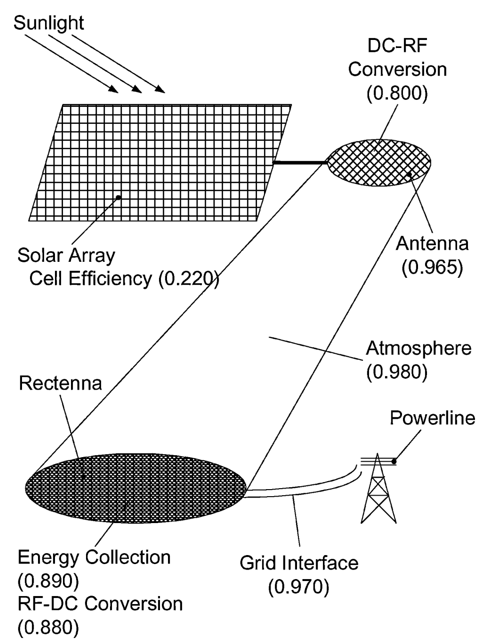

Fig. 6 Photovoltaic power generation system.

solar array is obtained from the following equation:

$$A_{sa} = H_{1sa}/C_s = 45.0 \times 10^3 \text{ m}^2 \tag{3}$$

Assuming that the solar array is rectangular, it is about 180 m wide and 250 m long.

As shown in Table 1, the antenna must transmit the energy per second $E_{a\text{PV}}$ of 6.72 MW. Assuming that the amount of transmittable energy per unit area perpendicular to the transmission direction is $C_a = 2.3$ kW/m^2, the cross-sectional area perpendicular to the transmission direction of the antenna is calculated by

$$A_{a\text{PV}} = E_{a\text{PV}}/\eta_a C_a = 3.03 \times 10^3 \text{ m}^2 \tag{4}$$

Assuming that the cross section perpendicular to the transmission direction of the antenna is circular, the diameter of the circle is

$$d_{a\text{PV}} = \sqrt{(4/\pi)A_{a\text{PV}}} = 62.1 \text{ m} \tag{5}$$

As evidenced in Table 1, the amount of waste heat per second of 51.8 MW that is the sum from the cell efficiency to aging degradation must be discarded from the power generation unit in this model, and the amount of waste heat per second of 3.12 MW must be disposed of at the power distribution unit and the power transmission unit.

SDPS Model

The concept of the SDPS is schematically shown in Fig. 7. The closed-Brayton-cycle (CBC) system,[5] shown in Fig. 8, is employed as the power generation unit in this model. The temperature at each point and the efficiencies of elements in the CBC are summarized in Table 2. The working fluid used in this model is a helium and xenon gas mixture. The properties of the working fluid are shown in Table 3.[14] The heat input per second at the receiver in the CBC system, the heat output per second from the gas cooler, and the efficiency of the cycle are calculated by using

$$H_{1\mathrm{CBC}} = \dot{m} c_{\mathrm{CBC}}(T_3 - T_6) \tag{6}$$

$$H_{2\mathrm{CBC}} = \dot{m} c_{\mathrm{CBC}}(T_5 - T_1) \tag{7}$$

$$\eta_{\mathrm{CBC}} = (H_{1\mathrm{CBC}} - H_{2\mathrm{CBC}})/H_{1\mathrm{CBC}} = 1 - (T_5 - T_1)/(T_3 - T_6) \tag{8}$$

The cycle efficiency in Table 2 is calculated from Eq. (8) and the temperatures at the points of the CBC listed in Table 4. Table 2 indicates that the heat input per second is $H_{1\mathrm{CBC}} = 29.9$ MW; thus, the mass flow rate of the working fluid in this cycle is obtained from

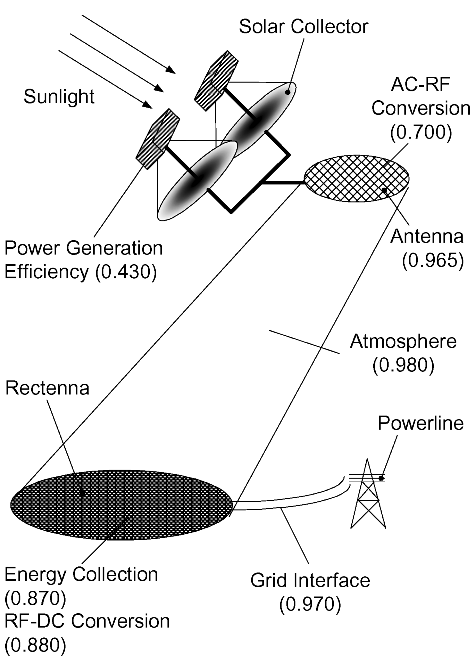

Fig. 7 Solar dynamic power generation system.

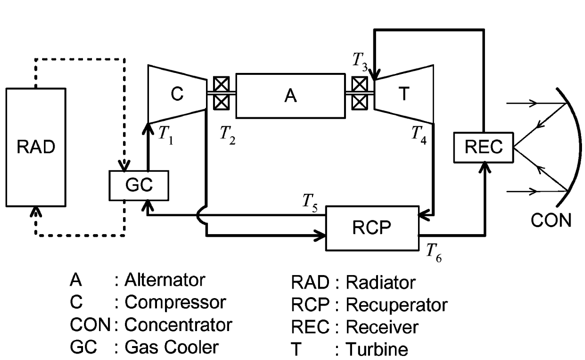

Fig. 8 Closed-Brayton-cycle system.

Table 2 System efficiency chain of SDPS

Item	Efficiency	Input energy, MW	Waste heat, MW
CBC cycle	0.430	29.86	17.03
Alternator	0.900	12.83	1.28
Power convertor and booster	0.950	11.55	0.58
Pantographic cables and distribution cables	0.990	10.97	0.11
Rotary joint	0.990	10.86	0.11
Power source of the transmission device	0.946	10.75	0.58
ac-rf conversion	0.700	10.17	3.05
Antenna	0.965	7.12	0.25
Atmosphere	0.980	6.87	0.14
Energy collection	0.870	6.73	0.88
rf-dc conversion	0.880	5.86	0.70
Grid interface	0.970	5.15	0.15
Powerline	——	5.00	——

Table 3 Properties of working fluid: He–Xe mixture gas

Parameter	Value
Molecular mass, g/mol	40
He, %	0.717
Specific heat C_{CBC}, KJ/kgK	0.519

Table 4 Temperatures and efficiencies of the CBC system

Parameter	Value
Compressor inlet temperature $T1$, K	290
Compressor outlet temperature $T2$, K	451
Turbine inlet temperature $T3$, K	1300
Turbine outlet temperature $T4$, K	960
Recuperator outlet temperature on higher-temperature side $T5$, K	527
Recuperator outlet temperature on lower-temperature side $T6$, K	884
Compressor pressure ratio, φ	2.50
Compressor efficiency, η_c	0.800
Turbine efficiency, η_t	0.850
Recuperator effectiveness, η_r	0.850

Eq. (6) as

$$\dot{m} = H_{1\mathrm{CBC}}/c_{\mathrm{CBC}}(T_3 - T_6) = 138 \text{ kg/s} \tag{9}$$

The cross-sectional area of the concentrator perpendicular to the rays of the sun is calculated by the following equation:

$$A_c = H_{1\mathrm{CBC}}/C_s = 21.8 \times 10^3 \text{ m}^2 \tag{10}$$

Assuming that the cross section perpendicular to the rays of the sun is circular, the diameter of the circle is

$$d_c = \sqrt{(4/\pi)A_c} = 167 \text{ m} \tag{11}$$

As shown in Table 2, the antenna must transmit the energy per second $E_{a\mathrm{SD}}$ of 6.87 MW. Assuming that the amount of transmittable energy per unit cross-sectional area perpendicular to the transmission direction is $C_a = 2.3$ kW/m^2, the cross-sectional area perpendicular to the transmission direction of the antenna is calculated by

$$A_{a\mathrm{SD}} = E_{a\mathrm{SD}}/\eta_a C_a = 3.10 \times 10^3 \text{ m}^2 \tag{12}$$

Assuming that the cross-sectional area perpendicular to the transmission direction of the antenna is circular, the diameter of the circle $d_{a\mathrm{SD}}$ is

$$d_{a\mathrm{SD}} = \sqrt{(4/\pi)A_{a\mathrm{SD}}} = 62.8 \text{ m} \tag{13}$$

As evidenced in Table 2, the amount of waste heat per second of 18.3 MW generated at the cycle and the alternator must be radiated from the power generation unit and the amount of waste heat per second of 4.68 MW generated from the power converter and booster to the antenna must be disposed of from the power distribution unit and the power transmission unit.

Design of Liquid Droplet Radiator

Flow Rate of Working Fluid

Considering that the temperature of the working fluid decreases by ΔT K during the flight in space between the droplet generator and the droplet collector, thermal energy lost per second of the working fluid is

$$\Delta H_{\mathrm{LDR}} = \rho_{\mathrm{LDR}} c_{\mathrm{LDR}} q \Delta T \tag{14}$$

Hence, the flow rate of the working fluid is calculated from

$$q = \frac{\Delta H_{\mathrm{LDR}}}{\rho_{\mathrm{LDR}} c_{\mathrm{LDR}} \Delta T} \tag{15}$$

The temperature drop ΔT is determined with the vapor pressure of the working fluid lower than 10^{-9} mm Hg to minimize the evaporation loss of the working fluid.[6]

Thickness, Width, and Length of the Droplet Sheet

Here, the concept of the optical depth normal to the surface of the droplet sheet is used. Because the optical depth represents the number of droplets included in a cylinder whose diameter is equal to the diameter of the droplet, the optical depth is obtained by

$$\tau = n\left(\pi d_d^2 \big/ 4\right) h \tag{16}$$

The number density of droplets is represented as

$$n = \left(f \big/ s_n^2 v_0\right) \tag{17}$$

It is known that the increase of the emissivity of the droplet sheet becomes small with the optical depth greater than two (Ref. 3). In this study, the optical depth is set at two. The thickness of the droplet sheet is determined by

$$h = 8 \big/ n \pi d_d^2 \tag{18}$$

The flow rate of the working fluid is represented by

$$q = n w h v_0 \cdot \tfrac{1}{6} \pi d_d^3 \tag{19}$$

Substituting Eq. (18) into Eq. (19) and rearranging for w yields

$$w = \frac{3q}{2\tau d_d v_0} \tag{20}$$

Considering that the total volume $dV(= whv_0 dt)$ of the droplets with temperature T travel the distance dx during time dt and increase in temperature by dT via radiative heat transfer, the following equation is satisfied:

$$-\rho_{\mathrm{LDR}} c_{\mathrm{LDR}} dV\, dT = 2\sigma \varepsilon_{\mathrm{sheet}} T^4 w\, dx\, dt \tag{21}$$

Dividing both sides by dt and integrating by separation of variables under the initial condition, $T = T_0$ at $x = 0$, the following equation is obtained:

$$\frac{1}{T^3} = \frac{6\varepsilon_{\mathrm{sheet}} \sigma w}{\rho_{\mathrm{LDR}} c_{\mathrm{LDR}} q} x + \frac{1}{T_0^3} \tag{22}$$

Under the initial conditions, when the working fluid is emitted from the droplet generator the temperature of the working fluid is T_0. Considering that the working fluid temperature decreases by ΔT during the flight of length l from the droplet generator to the droplet collector, $T = T_0 - \Delta T$ at $x = l$, and the length is obtained by

$$l = \frac{\rho_{\mathrm{LDR}} c_{\mathrm{LDR}} q}{6\varepsilon_{\mathrm{sheet}} \sigma w}\left[\frac{1}{(T_0 - \Delta T)^3} - \frac{1}{T_0^3}\right] \tag{23}$$

Table 5 Properties of working fluid (silicon oil)

Parameter	Value
Density ρ, kg/m^3	957
Coefficient of viscosity μ, Pa · s	0.0479
Surface tension σ, N/m	0.0208

Table 6 Generation condition of droplets and characteristics of the generated droplets

Parameter	Value
Nozzle diameter D, μm	100
Pressure difference between the inside and the outside of the orifice ΔP, MPa	0.30
Frequency of pressure disturbance f, kHz	12
Nondimensional wave number k	0.362
Droplet velocity v_0, m/s	10.4
Droplet diameter d_d, μm	235
Spacing between droplets s_d, μm	198

Droplet Velocity

For the nozzle used in our experiments, it has been clarified that the droplet velocity v_0 is expressed by[10]

$$v_0 = -\left[\left(\frac{64\nu_{\mathrm{LDR}} L}{D^2} + \frac{\xi \nu_{\mathrm{LDR}} L}{a D^2}\right) + \sqrt{\left(\frac{64\nu_{\mathrm{LDR}} L}{D^2} + \frac{\xi \nu_{\mathrm{LDR}} L}{a D^2}\right)^2 + \frac{8\Delta P}{\rho_{\mathrm{LDR}}}}\,\right] \Bigg/ 2 \tag{24}$$

The diameter of the nozzle, the difference between the upward and the downward pressure of the nozzle, and the frequency of pressure disturbance are designed in such a way that the growth factor is approximately the maximum value at which a uniform droplet stream can be emitted from the droplet generator. As shown in Fig. 4, the growth factor is a maximum value in the vicinity of the nondimensional wave number of 0.35 when the working fluid is silicon oil (Shin-Etsu Chemical Co., Ltd., KF-96 50 cSt) and the diameter of the nozzle is $D = 100\ \mu$m. The properties of this silicon oil are listed in Table 5. The diameter of the nozzle, the pressure difference, and the frequency of pressure disturbance are shown in Table 6. The droplet velocity, the droplet diameter, and the droplet spacing are calculated from Eqs. (1), (2), and (22), respectively, and are shown in Table 6.

Results and Discussion

LDR for the PVPS Model

Power Generation Unit

As shown in Table 1, 51.8 MW of waste heat per second at the solar array H_{sa} must be disposed of at the power generation unit in this model. Assuming that the total amount of waste heat is discarded by radiative heat transfer from both sides of the solar array, the following equation is satisfied:

$$2\varepsilon_{\mathrm{sa}} \sigma T_{\mathrm{sa}}^4 A_{\mathrm{sa}} = H_{\mathrm{sa}} \tag{25}$$

Solving this equation for T_{sa} gives

$$T_{\mathrm{sa}} = 333\ \mathrm{K} \tag{26}$$

This equation means that the solar array attains equilibrium at the temperature of 333 K. Hence it is clear that the power generation unit does not require any active cooling system. In the case of condensing sunlight with the reflector:

$$2\varepsilon_{\mathrm{sa}} \sigma T_{\mathrm{sa}}^4 (A_{\mathrm{sa}}/C_r) = H_{\mathrm{sa}} \tag{27}$$

Table 7 Characteristics of the LDR for power distribution unit and power transmission unit of PVPS

Parameter	Value
Waste heat per second, MW	3.05
Temperature of droplets in the sheet, K	300–285
Flow rate of the working fluid, m^3/s	0.141
Length of the sheet, m	107
Width of the sheet, m	43.2
Thickness of the sheet, m	0.998
Optical depth	2
Effective emissivity of the sheet	0.80
Number density of droplets, $1/m^3$	4.61×10^7
Spacing between nozzles, mm	5.00

Assuming that the upper allowable flight temperature limit of the solar cell is 353.15 K,

$$C_r = 1.34 \tag{28}$$

Therefore, a power generation unit with reflectors whose concentration ratio is higher than 1.34 requires an active cooling system.

Power Distribution Unit and Power Transmission Unit

As shown in Table 1, the total amount of waste heat per second $H_{\mathrm{d-t\ PV}}$ of 3.12 MW must be removed from the power distribution unit and the power transmission unit in this model. Assuming that part of the waste heat is disposed of by radiative heat transfer from both sides of the antenna and setting the surface temperature of both sides at $T_a = 333$ K, the LDR for the power distribution unit and the power transmission unit must dispose of the following amount of waste heat per second:

$$\begin{aligned} H_{\mathrm{LDR\,d-t}} &= H_{\mathrm{d-t\ PV}} + \varepsilon_a C_s A_{a\mathrm{PV}} - 2\varepsilon_a \sigma T_a^4 A_{a\mathrm{PV}} \\ &= 3.05\,\mathrm{MW} \end{aligned} \tag{29}$$

where the emissivity of both sides of the antenna is 0.8.

The upper limit of the permissive temperature range of these units is about 60°C (= 333 K) because they include electrical parts. The temperature of the waste heat from these parts is also lower than 333 K. Silicon oil is suitable as the working fluid of the LDR for cooling these units. The characteristics of the LDR, with the working fluid of silicon oil, for these units of the PVPS are summarized in Table 7. It is clear that the LDR with a droplet sheet 107 m long, 43.2 m wide, and 0.998 m thick is required for the power distribution unit and the power transmission unit.

LDR for the SDPS model

Power Generation Unit

As shown in Table 2, the amount of waste heat per second H_c of 18.3 MW generated at the cycle and the alternator must be removed from the power generation unit (CBC and alternator) in this model. Assuming that the waste heat is disposed of by radiative heat transfer from the back of the reflective surface of a concentrator, the following equation is satisfied:

$$\varepsilon_c \sigma T_c^4 A_c = H_c \tag{30}$$

where the emissivity of the back of the reflective surface of a concentrator is 0.8. Solving this equation for T_c gives

$$T_c = 374\,\mathrm{K} = 101°\mathrm{C} \tag{31}$$

This equilibrium temperature is beyond the permissible temperature of the control unit of the concentrator. Assuming that part of the waste heat is disposed of by radiative heat transfer from the back of the reflective surface of the concentrator and setting the surface temperature of the back at $T_c = 333$ K, the LDR for the power generation unit must dispose of the following amount of waste heat per second:

$$H_{\mathrm{LDR\,SD}} = H_c - \varepsilon_c \sigma T_c^4 A_c = 6.13\,\mathrm{MW} \tag{32}$$

Table 8 Characteristics of the LDR for the power generation unit of SDPS

Parameter	Value
Waste heat per second, MW	6.13
Temperature of droplets in the sheet, K	300–280
Flow rate of the working fluid, m^3/s	0.170
Length of the sheet, m	147
Width of the sheet, m	65.1
Thickness of the sheet, m	0.998
Optical depth	2
Effective emissivity of the sheet	0.08
Number density of droplets, $1/m^3$	4.61×10^7
Spacing between nozzles, mm	5.00

Table 9 Characteristics of the LDR for the power distribution unit and the power transmission unit of SDPS

Parameter	Value
Waste heat per second, MW	4.61
Temperature of droplets in the sheet, K	300–285
Flow rate of the working fluid, m^3/s	0.213
Length of the sheet, m	107
Width of the sheet, m	65.2
Thickness of the sheet, m	0.998
Optical depth	2
Effective emissivity of the sheet	0.80
Number density of droplets, $1/m^3$	4.61×10^7
Spacing between nozzles, mm	5.00

The working fluid temperature decreases from 527 to 290 K at the gas cooler of the CBC. Silicon oil is again adequate as the working fluid. The characteristics of the LDR with the working fluid of silicon oil for this unit of the SDPS are shown in Table 8. It is clear that the LDR with a droplet sheet 147 m long, 65.1 m wide, and 0.998 m thick is required for the power generation unit. The farther the droplet collector is separated from the droplet generator, the longer the length of the droplet sheet is. Considering that the full 60-m mast was successfully deployed from the payload bay to one side of the shuttle in the Shuttle Radar Topography Mission[15] in February 2000, it is estimated that a 147-m length of the droplet sheet can be constructed using existing technology and deployment from both sides of a structure.

Power Distribution Unit and Power Transmission Unit

As shown in Table 2, the total amount of waste heat per second of 4.68 MW must be removed from the power distribution unit and the power transmission unit in this model. Calculating the amount of waste heat that must be removed by the LDR for the power distribution unit and the power transmission unit in the same manner as the PVPS, we obtain

$$H_{\mathrm{LDR}\,d\text{-}t} = 4.61\,\mathrm{MW} \tag{33}$$

The characteristics of the LDR with silicon oil as the working fluid for these units of the SDPS are summarized in Table 9. It is clear that an LDR with a droplet sheet 107 m long, 65.2 m wide, and 0.998 m thick is required for the power distribution unit and the power transmission unit.

Conclusions

In the present work, the waste heat from a space solar-power system (SPS), which feeds 5 MW to a power transmission line on Earth, and its removal by liquid droplet radiators have been considered. The quantitative study of liquid droplet radiators has been performed on the basis of the results of experiments carried out under microgravity. Two power generation systems, the photovoltaic power system (PVPS) and the solar dynamic power system (SDPS), have been considered as models of SPS. The following results have been obtained. First, although the amount of waste heat from the power generation unit in the PVPS is 51.8 MW, a heat removal system is not necessary when the concentration ratio of solar energy is less than 1.34 because the waste heat is fully dissipated from the surface of the photovoltaic solar array. Second, the heat removal system must dispose of 18.3 MW of waste heat from the power generation unit in the SDPS. Third, the total amount of waste heat from the power distribution unit and the power transmission unit is 3.12 MW in the PVPS and 4.68 MW in the SDPS. Fourth, the droplet sheet of the LDR for radiating energy, in which the working fluid is silicon oil, must be 147 m long, 65.1 m wide and 0.998 m thick in order to effectively manage the waste heat from the power generation unit in the SDPS. Fifth, the droplet sheet of the liquid droplet radiator (LDR) for radiating energy, in which the working fluid is silicon oil, must be 107 m long, 43.2 m wide, and 0.998 m thick in order to effectively manage the waste heat from the power distribution unit and the power transmission unit in the PDPS, and 107 m long, 65.2 m wide, and 0.998 m thick in the SDPS.

It is easily understood from these results that the construction of the LDR for the SPS, which feeds only 5 MW to a power transmission line on Earth, is high in cost. Advanced technologies such as inflatable deployment technology and a less expensive transport system into space are necessary in order to be able to construct the LDR in orbit at a low cost. Nonetheless, it is noteworthy that the LDR for a SPS, which feeds 5 MW to a power transmission line on Earth, can be constructed by using existing technology.

References

[1]Glaser, P. E., "Power from the Sun: Its Future," *Science*, Vol. 162, No. 3856, 1968, pp. 857–861.

[2]Mankins, J. C., "A Fresh Look at Space Solar Power: New Architectures, Concepts and Technologies," *Acta Astronaoutica*, Vol. 41, Nos. 4–10, 1997, pp. 347–359.

[3]Mattick, A. T., and Hertzberg, A., "Liquid Droplet Radiators for Heat Rejection in Space," *Journal of Energy*, Vol. 5, No. 6, 1981, pp. 387–393.

[4]Taussig, R. T., and Mattick, A. T., "Droplet Radiator Systems for Spacecraft Thermal Control," *Journal of Spacecraft and Rockets*, Vol. 23, No. 1, 1986, pp. 10–17.

[5]Massardo, A. F., Tagliafico, L. A., Fossa, M., and Agazzani, A., "Solar Space Power System Optimization with Ultralight Radiator," *Journal of Propulsion and Power*, Vol. 13, No. 4, 1997, pp. 560–564.

[6]Presler, A. F., Coles, C. E., Diem-Kirsop, P. S., and White, K. A., "Liquid Droplet Radiator Program at the NASA Lewis Research Center," American Society of Mechanical Engineers, ASME 86-HT-15, June 1986.

[7]White, K. A., "Liquid Droplet Radiator Development Status," AIAA Paper 87-1537, June 1987.

[8]Hosokawa, S., Kawada, M., Iwasaki, A., and Kudo, I., "Formation of a Uniform Liquid Droplet Stream for a Liquid Droplet Radiator," *Journal of the Japan Society for Aeronautical and Space Sciences*, Vol. 39, No. 453, 1991, pp. 551–557 (in Japanese).

[9]Hosokawa, S., Kawada, M., Iwasaki, A., and Kudo, I., "Observation of Collecting Process of Liquid Droplets in Liquid Droplet Radiator," *Journal of the Japan Society for Aeronautical and Space Sciences*, Vol. 41, No. 474, 1993, pp. 385–390 (in Japanese).

[10]Totani, T., Itami, M., Yabuta, S., Nagata, H., Kudo, I., Iwasaki, A., and Hosokawa, S., "Performance of Droplet Emittor for Liquid Droplet Radiator under Microgravity," *Transactions of the Japan Society of Mechanical Engineers B*," Vol. 68, No. 668, 2002, pp. 1166–1173 (in Japanese).

[11]Totani, T., Itami, M., Nagata, H., Kudo, I., Iwasaki, A., and Hosokawa, S., "Performance of Droplet Generator and Droplet Collector in Liquid Droplet Radiator Under Microgravity," *Microgravity Science and Technology*, Vol. 13, No. 2, 2002, pp. 42–45.

[12]Dixon, M., "Droplet Velocity Dispersion Device," AIAA Paper 85-0077, Jan. 1985.

[13]Hanley, G. M., "Satellite Power Systems (SPS) Concept Definition Study (Exhibit D)," NASA CR 3393, Vol. 2, March 1981.

[14]Pietsch, A. A., and Trimble, S. W., "Closed Brayton Solar Dynamic Power for the Space Station," International Astronautical Federation, IAF-86-135, Oct. 1986.

[15]Rabus, B., Eineder, M., Roth, A., and Bamler, R., "The Shuttle Radar Topography Mission—a New Class of Digital Elevation Models Acquired by Spaceborne Radar," *ISPRS Journal of Photogrammetry and Remote Sensing*, Vol. 57, No. 4, 2003, pp. 241–262.

N. Gatsonis
Associate Editor